# Induced Super-Halogen Behavior of Metal Moieties in Halogen-Doped Clusters: LinI(-) and AlnI(-), n = 13, 1, 2, 3

**ARTICLE** *in* THE JOURNAL OF PHYSICAL CHEMISTRY A · APRIL 2007

Impact Factor: 2.69 · DOI: 10.1021/jp0631937 · Source: PubMed



**2 AUTHORS**, INCLUDING:

Fedor Y. Naumkin
University of Ontario Institute of Technology

**64** PUBLICATIONS **659** CITATIONS

SEE PROFILE

# Induced Super-halogen Behavior of Metal Moieties in Halogen-Doped Clusters: $Li_nI^{(-)}$ and $Al_nI^{(-)}$, $n = 13, 1, 2, 3$

**Hobart Leung and Fedor Y. Naumkin***

*Faculty of Science, University of Ontario Institute of Technology, Oshawa, Ontario L1H 7K4, Canada*

*Received: May 24, 2006; In Final Form: October 6, 2006*

A comparative density functional theory (DFT) study of a series of neutral and negative-ionic lithium and aluminum clusters doped with iodine atom is presented. The I atom is found to preserve the same position at $Li_{13}$ with and without the negative charge and $Li_{13}$ to vary its shape from prolate to oblate with changing spin state of $Li_{13}I$. Both the Mulliken and natural charges are considered, the natural-charge separation between the metal and halogen moieties being generally much larger (except for $Al_{13}I^-$). In $Li_nI^-$, the additional electron is strongly localized on the metal moiety starting from $n = 1$, even though the electron affinity of $Li_n$ is much smaller than that of I. Such a super-halogen behavior of $Li_n$ is induced by highly electronegative iodine making the two components charged in $Li_nI$ and leading to a charge−dipole interaction with the additional electron. In $Al_nI^-$, similar factors result in $Al_n$ being more negative than I already for $n = 3$, even though the electron affinity of I is higher, the effect escalating for $n = 13$.

## Introduction

Metal clusters have been intensely studied as intermediates between the individual atoms and bulk metals, in order to track the evolution of properties with an increasing amount of matter. Since the clusters have exhibited a unique behavior, such as nonmetallic character when being sufficiently small, or increased stability and extrema in other parameters (ionization potentials, electron affinities, etc.) at specific ("magic") sizes, they have become objects of interest by themselves.[1] Their modern areas of application include new materials, catalysis, molecular electronics/photonics, and others.

Among the unusual properties of some metal clusters is a high electron affinity (EA) comparable to or even exceeding that of halogen atoms, as found, for instance, for $Al_{13}$ [2] and attributed to the closed electronic shell (with 40 valence electrons) of the cluster negative ion, $Al_{13}^-$. The neutral $Al_{13}$ cluster has therefore been named "super-halogen" and proposed as a potential building unit for new materials. For instance, it might be incorporated as a cluster analogue of an electronegative atom in an ionic crystal. Other examples include, in particular, pure and doped gold clusters such as $Au_{13}$ [3] and $MAu_{12}$ (M = V, Nb, Ta) [4]. Earlier notions of super-halogens include theoretical predictions for Groups I−V atom super-halides,[5] verified experimentally for the Group I and II cases.[6,7]

The EA value of $Al_{13}$ higher than that of I has also been referred to in interpreting the charge distribution in $Al_{13}I^-$, with the negative charge located mainly on the metal moiety.[8] Moreover, the charge in $Al_{13}I^-$, according to the HOMO density, concentrates on the Al atom remotest from I. The latter feature, however, would not seem to follow from the relative EA values of the two components, but would rather fit the dipole field of the neutral metal−halogen system interacting with the additional electron.

The aim of this work is to investigate the origins of the above charge distribution and to try to understand what other factors may be responsible for its features, in addition to the relative EA values of the constituent metal-cluster and halogen atom in the metal−halide cluster ions. For this purpose, one could consider another metal cluster, with EA lower relative to the halogen's, and compare its behavior in a halide compound similar to that of $Al_{13}$. Alkali metals are ultimate "non-halogens", so, for instance, $Li_{13}$ is a reasonable candidate, whose similar closed-shell atomic but different open-shell electronic structure would make the comparison adequate. Besides, the $Li_{13}I$ system has 20 valence electrons and is therefore also interesting as a closed-shell species. Further, it is logical to look at smaller counterparts such as $M_nI^-$ (M = Li, Al; $n = 1, 2, 3$) in order to check how the charge-distribution features evolve with the cluster size, as small $M_n$ are known to be no super-halogens. The results of these studies are presented below.

## Computational Procedure

Present calculations have been performed with the NWChem ab initio package [9] and pictures generated using the Molekel software.[10] For a consistent comparison with previous work,[8] density functional theory (DFT) has been employed. The PBE0 functional, which showed a good performance for aluminum clusters,[11] was used. The cc-pVDZ basis set for Li and Al atoms and the LANL2DZ effective core potential plus corresponding basis set for the I atom (incorporated into NWChem) have been used. Neutral and ionic system geometries have been optimized for the low-energy electronic states with a few spin multiplicities. The optimization has involved all atoms and been done in the $C_1$ symmetry group in order to avoid additional geometry constraints able to lead to incorrect predictions of stable geometries.

Results of test calculations at this level of theory are compared in Table 1 with experimental data taken from a National Institute of Standards and Technology (NIST) online database.[12] As can be seen, the comparison is favorable for relevant atomic as well as diatomic species, the deviations not exceeding 3% in both characteristic energies and distances, except for $D_e$ of metal

* To whom correspondence should be addressed. E-mail: fedor.naumkin@uoit.ca.

10.1021/jp0631937 CCC: $33.50 
Published on Web 11/30/2006

**TABLE 1: Comparison of Calculated and Experimental Atomic and Diatomic Parameters**

| system | calculation | experiment[12] |
|---|---|---|
| I | EA = 3.03 eV | 3.06 eV |
| Li | IE = 5.57 eV | 5.39 eV |
| LiI | $D_e$ = 3.66 eV | 3.56 eV [a] |
| | $R_e$ = 2.44 Å | 2.39 Å |
| $Li_2$ | $D_e$ = 0.83 eV | 1.07 eV [a] |
| | $R_e$ = 2.74 Å | 2.67 Å |
| Al | IE = 6.10 eV | 5.99 eV |
| AlI | $D_e$ = 3.80 eV | 3.84 eV [a] |
| | $R_e$ = 2.59 Å | 2.54 Å |
| $Al_2$ | $D_e$ = 1.45 eV | 1.63 eV [a] |
| | $R_e$ = 2.49 Å | 2.47 Å |

[a] $D_e \approx D_0 + h\omega_e/2$.

diatoms, underestimated by 10−20%. The latter deviation is, however, not crucial for this work.

## Results and Discussion

**$Li_{13}I$.** The $Li_{13}$ cluster has previously been found (see, for instance, ref 10) to adopt icosahedral geometry in its ground state, similar to the $Al_{13}$ cluster. When the I atom is attached, its most stable position is predicted to be at the hollow site, above the center of the triangular unit of $Li_{13}$ (Figure 1a), unlike the bridging position between two surface atoms of $Al_{13}$.[8] It should be noted here that later studies[14] have found a low-symmetry structure of $Al_{13}I$ to be lower in energy by ≈0.2 eV. However, it corresponds to a non-icosahedral shape of the $Al_{13}$ moiety, while it is interesting to make a comparison of systems with the metal components similar in shape. In this work we will therefore consider the above (bridge) low-energy isomer of $Al_{13}I$ which (approximately) preserves the icosahedral $Al_{13}$ moiety. Its difference in the I position from $Li_{13}I$ can be related to the directional character of the valence p-orbital of Al as compared to the isotropic s-orbital of Li, affecting the overlap with the p-orbital of I.

The lowest-energy state of $Li_{13}I$ is predicted to be triplet, followed by quintet only 0.08 eV higher, while singlet is 0.52 eV above the (triplet) ground state. This is to be correlated with the $Li_{13}$ sextet ground state and the quartet state ≈1.2 eV above. The ground-state I-nearest Li distances in $Li_{13}I$ are calculated to be ≈0.3 Å longer relative to that in the LiI diatom (Table 2), which could be expected in terms of a reduced overlap of the Li s-orbital and I p-orbital (not pointing directly to Li). The $Li_{13}$ moiety is slightly elongated in the direction to iodine, with the distances between the opposite Li atoms (through the center of the cluster) being 6.0 ± 0.1 Å, which is ≈0.2 Å longer than for such distances in the (approximately) perpendicular direction. The energy for detaching the iodine is found to be ≈0.4 eV larger compared to that for LiI (Table 2), apparently as a result of interaction with more than one lithium (at least three nearest).

It is interesting that, for the singlet state, the $Li_{13}$ moiety is somewhat compressed along the direction to I, as is visible in Figure 1b, with the through-center Li−Li distances of 5.69 Å, significantly shorter (by 0.54 Å) than in the perpendicular direction. The quintet state, in turn, corresponds to the $Li_{13}$ moiety more spherical, with the distances between the opposite Li atoms within 5.9 ± 0.1 Å. The I-nearest Li distances are almost unchanged from the ground state, at 2.76 ± 0.03 Å for both singlet and quintet.

Charge distributions have been evaluated in terms of both the Mulliken and the natural charges on atoms (from the natural atomic and bond orbital analysis), the latter values being presented hereafter by default. The results for the ground state are collected in Table 3 and indicate a negative charge on the I atom, as expected, from both approaches, the Mulliken value being much smaller.

It should be noted that at present the natural-charge values are commonly considered as more reliable since they are much less sensitive to the basis set. Another, more specific reason relevant to this work is the unreasonably high Mulliken charges on the internal atoms of metal clusters, for instance central atoms of icosahedral 13-atom systems.[15] In particular for the present case of $Li_{13}I$, the (positive) Mulliken charge on $Li_{central}$ of the $Li_{13}$ moiety is found to exceed the Li-nucleus charge. On the other hand, the natural charge on $Li_{central}$ is negative (−0.65 e). Similar method-related features of the charge distribution are obtained for isolated $Li_{13}$ as well (with the natural charge of −0.52 e on $Li_{central}$). Such a concentration of the electron density in the center of a metal cluster seems to be rather counterintuitive, even taking into account the cluster's possible nonmetallic character at such a small scale.

In terms of the natural charges, three Li atoms nearest to I and thus between the two negative centers carry most of the positive charge, +0.93 e (Figure 1a), followed by a ring of six peripheral Li atoms less positive and then by three lithiums (most remote from I) still more weakly charged. The $Li_{13}$ moiety in $Li_{13}I$ is thus strongly polarized due to I. Interestingly, the higher-energy singlet state exhibits a layered alternate-sign charge distribution (Figure 1b) with the charge on the 3-Li unit near I reaching +1.45 e, followed by a negatively charged 6-atom ring at −0.78 e around the central atom (with −0.58 e), and then by the 3-Li unit most remote from I with +0.67 e charge. The corresponding Mulliken distribution, on the other hand, shows the near-I three lithiums most negative and no charge-layers instead.

In the present work, of main concern is the charge separation between the iodine and lithium moieties. Such a property is directly related to the system dipole moment. Its ab initio value is ≈2.8 D (for either the ground or the singlet state), and the direction is in accord with the positively charged metal moiety.

**$Li_{13}I^-$.** When another electron is added to $Li_{13}I$, the lowest-energy structure still has iodine at the hollow site (Figure 1c), compared to the (changed) position on top of a single metal atom in $Al_{13}I^-$ [8]. This can be looked at, in a simplistic way, as $I^-$ sphere (in terms of unperturbed electron density) lying comfortably between three other Li spheres. The ground state is predicted to be sextet, with the quartet and doublet only 0.075 and 0.12 eV above. The ground-state I-nearest Li distances slightly stretch (within 0.1 Å, Table 2) relative to the neutral counterpart, consistent with increasing internuclear distance in $LiI^-$ relative to LiI, and is essentially invariant (within 0.01 Å) for quartet and doublet. The $Li_{13}$ moiety is almost symmetric for all spin states, with only minor compression or elongation in the direction to I (within 0.1 Å) and is essentially of the same size (about 5.9 Å in diameter) as in the neutral system. The binding energy of $I^-$ to $Li_{13}$ is ≈1.1 eV larger than for $LiI^-$, and ≈1.6 eV smaller than for $Li_{13}I$ (Table 2), similar to its reduction for $LiI^-$ relative to LiI. For both the neutral and ionic clusters, this binding energy is relative to the lowest-energy sextet state of $Li_{13}$.

The electron affinity of $Li_{13}I$ is predicted to be 1.47 eV, intermediate between ≈3 eV for I and 0.92 eV of $Li_{13}$ (with the latter obtained relative to the lowest-energy quintet state of $Li_{13}^-$). This indicates that the additional electron in $Li_{13}I^-$ is significantly delocalized between the metal cluster and iodine.

Indeed, the charge on I increases only slightly in $Li_{13}I^-$ relative to $Li_{13}I$ (Table 3), according to both the Mulliken and

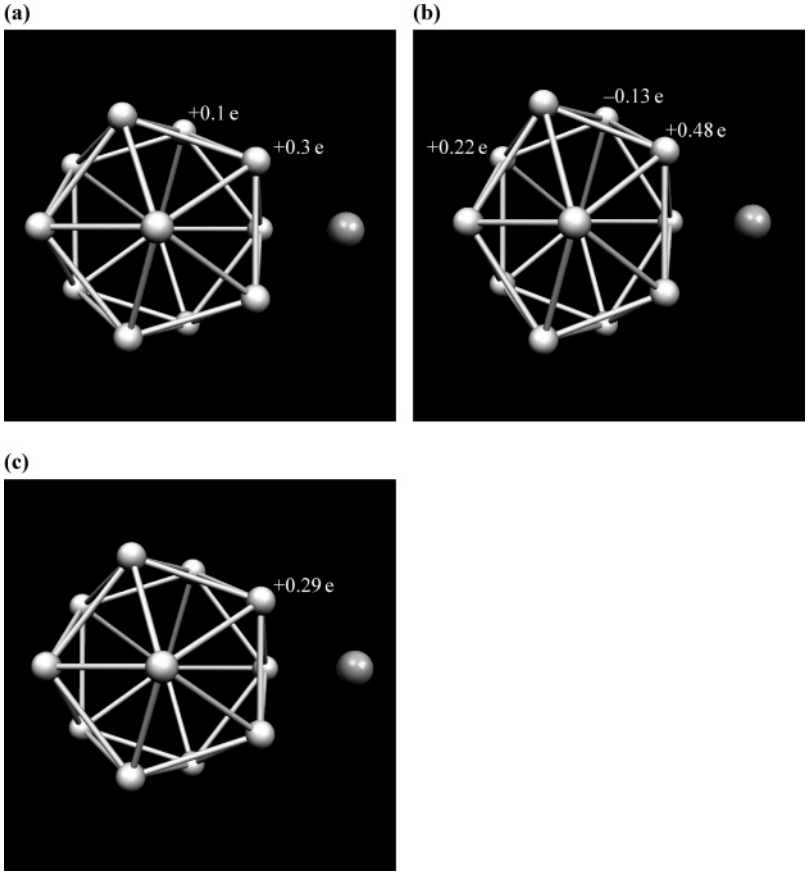


**Figure 1.** Optimized geometries and atomic natural charges of $Li_{13}I$ (a) triplet and (b) singlet and (c) $Li_{13}I^-$ sextet.

**TABLE 2: Calculated Equilibrium Parameters of the Ground-State Systems**

| system, $M_nI^{(-)}$ | $D_e(M_n{:}I^{(-)})$/eV | $R_e$(M:I)/Å |
|---|---|---|
| $Li_{13}I$ | 4.08 | 2.73−2.76 |
| $Li_{13}I^-$ | 2.51 | 2.80 |
| $Li_2I$ (T-shaped) | 3.84 | 2.63 |
| $Li_2I^-$ (T-shaped) | 1.44 | 2.69 |
| $Al_2I$ (T-shaped) | 3.56 | 2.86 |
| $Al_2I^-$ (T-shaped) | 1.54 | 3.03 |
| $Al_3I$ | 3.20 | 2.52 |
| $Al_3I^-$ | 2.15 | 2.66 |
| $Al_{13}I$ | 2.8 | 2.79−2.84 |
| $Al_{13}I^-$ | 3.03, 2.49 [a] | 2.58 |

[a] $D_e(I{:}Al_{13}^-)$

natural values, so that most of the additional-electron charge (>90%) goes to the $Li_{13}$ moiety, making it negatively charged. The negative charge already present on I in the neutral system thus largely *remains* on iodine in the ionic system, and the additional electron is attracted almost entirely to the positively charged lithium cluster within $Li_{13}I$, consistent with a simple electrostatic picture of the charge−dipole interaction. The EA value of $Li_{13}I$, much closer to that for $Li_{13}$ than for I, also confirms that it is the metal moiety which accommodates the additional electron.

The natural charge on the central atom of the $Li_{13}$ moiety increases to −0.92 e in $Li_{13}I^-$. In the isolated $Li_{13}^-$, by comparison, this charge is reduced (to −0.38 e) relative to the neutral cluster, so the presence of I has a substantial effect on the charge distribution. The three Li atoms nearest to I remain positively charged (+0.86 e altogether) in $Li_{13}I^-$, while the rest of the atoms are essentially neutral (Figure 1c).

It is worth emphasizing that the low and high EA values of isolated $Li_{13}$ and I, respectively, are thus not the main factors affecting the additional-electron preferred location on $Li_{13}$. This location is actually determined by the respectively high and low effective electron affinities of the metal and halogen moieties having ionic characters ($Li_{13}^{\delta+}$ and $I^{\delta-}$) inside $Li_{13}I$. The $Li_{13}$ cluster, no super-halogen in terms of its EA value, therefore exhibits a super-halogen behavior (by winning the additional electron from I) within $Li_{13}I$, and this behavior is induced by iodine. The effect is even more dramatic in terms of the Mulliken charges showing that most of the negative charge in $Li_{13}I^-$ is on $Li_{13}$ (Table 3), with a similar result obtained previously for $Al_{13}$ in $Al_{13}I^-$.[8]

**Model.** A simple model supporting the above considerations can be suggested as follows. Consider a partially charged species (within a system) as a formal combination of its purely neutral and purely ionic forms, with the ionic character determined by the (absolute) charge value; i.e., $A^{\delta\pm} \approx (1-\delta)A + \delta A^{\pm}$. If we adopt the ionization energy IE of the neutral species as EA of the corresponding positive ion, then

$$EA(Li_{13}^{\delta+}) \approx (1-\delta)EA(Li_{13}) + \delta EA(Li_{13}^{+}) = (1-\delta)EA(Li_{13}) + \delta IE(Li_{13})$$

$$EA(I^{\delta-}) \approx (1-\delta)EA(I) + \delta EA(I^-)$$

From the second equation it is clear that the higher the negative charge on the halogen moiety, the less electronegative it will be, as the Coulomb repulsion of the additional electron from the negative ion can even make its EA negative. Indeed, calculation at the same level of theory as before gives the energy of $I^{2-}$ as 19.5 eV above that for $I^-$, so that we can put $EA(I^-) \approx -19.5$ eV for our purpose. It is worth noting that we do not put $EA(I^-) = 0$, since this would omit the actually present repulsion of the additional electron from $I^{\delta-}$ in $Li_{13}I$. In other

**TABLE 3: Charges (in e) on the Lithium and Iodine Moieties in the Ground-State Systems**

| method | $Li_nI$ | $Li_nI^-$ | difference (additional electron) |
|---|---|---|---|
| Mulliken | $q(Li_{13})/q(I) = \pm 0.09$ | $-0.82/-0.18$ | $-0.91/-0.09$ |
| | $q(Li)/q(I) = \pm 0.32$ | $-0.41/-0.59$ | $-0.73/-0.27$ |
| | $q(Li_2)/q(I) = \pm 0.15$ | $-0.75/-0.25$ | $-0.90/-0.10$ |
| natural | $q(Li_{13})/q(I) = \pm 0.77$ | $-0.20/-0.80$ | $-0.97/-0.03$ |
| | $q(Li)/q(I) = \pm 0.85$ | $-0.09/-0.91$ | $-0.94/-0.06$ |
| | $q(Li_2)/q(I) = \pm 0.83$ | $-0.11/-0.89$ | $-0.94/-0.06$ |

**TABLE 4: Charges (in e) on the Aluminum and Iodine Moieties in the Ground-State Systems**

| method | $Al_nI$ | $Al_nI^-$ | difference (additional electron) |
|---|---|---|---|
| Mulliken | $q(Al_{13})/q(I) = \pm 0.05$ | $-0.72/-0.28$ | $-0.77/-0.23$ |
| | $q(Al)/q(I) = \pm 0.21$ | $-0.44/-0.56$ | $-0.65/-0.35$ |
| | $q(Al_2)/q(I) = \pm 0.17$ | $-0.44/-0.56$ | $-0.61/-0.39$ |
| | $q(Al_3)/q(I) = \pm 0.14$ | $-0.61/-0.39$ | $-0.75/-0.25$ |
| natural | $q(Al_{13})/q(I) = \pm 0.13$ | $-0.68/-0.32$ | $-0.81/-0.19$ |
| | $q(Al)/q(I) = \pm 0.55$ | $-0.29/-0.71$ | $-0.84/-0.16$ |
| | $q(Al_2)/q(I) = \pm 0.49$ | $-0.43/-0.57$ | $-0.92/-0.08$ |
| | $q(Al_3)/q(I) = \pm 0.30$ | $-0.54/-0.46$ | $-0.84/-0.16$ |

words, we should not conclude that electron will fly away from $I^-$ as it likely would from isolated $I^-$, since in the former case the electron is kept in the system by $Li_{13}^{\delta+}$. Besides, the use of the limited basis set for $I^{2-}$, lacking diffuse functions (hence effectively confining the electron close to the ion), is consistent, as it is this basis set which is used to describe the total system ($Li_{13}I^-$) and its relevant component ($I^{\delta-}$).

Taking the $\delta$ value from Table 3, we obtain $EA(I^{\delta-}) \approx 1.0$ and $-14$ eV for the Mulliken and natural charges, respectively. Since $EA(Li_{13}^{\delta+})$ is to be positive anyway, the natural-charge based result already implies the additional electron's strong preference of the metal moiety. The ionized $Li_{13}^+$ cluster has been optimized at the same level of theory for a few spin states and the quintet found to be the ground state. The calculated $IE(Li_{13}) = 4.85$ eV in combination with the above-mentioned $EA(Li_{13}) = 0.92$ eV results in $EA(Li_{13}^{\delta+}) \approx 1.3$ and 4.0 eV for the Mulliken and natural charges, respectively. As can be seen, the charges on the metal and halogen moieties within the cluster can indeed affect their electronegativities considerably.

It should be noted that in the earlier discussion EA of $Li_{13}I$ has been compared to those of neutral rather than charged metal and halogen moieties. This, however, does not affect the conclusion: the value for the cluster is still much closer to $EA(Li_{13}^{\delta+})$ than to $EA(I^{\delta-})$, for both Mulliken and natural charges. The reason is the larger difference between the EA values for the neutral iodine and for the charged iodine moiety, as a result of the much larger difference between EA(I) and $EA(I^-)$ than between EA(Li) and $EA(Li^+)$.

Besides, the $EA(Li_{13}I)$ value remains between EA for $Li_{13}^{\delta+}$ and $I^{\delta-}$ because they are respectively larger and lower compared to those for $Li_{13}$ and I. Similar considerations apply also to other species below.

**LiI and $Li_2I$.** At this stage, it is interesting to check if similar features can be found for smaller counterparts such as LiI and $Li_2I$. For consistency, calculations for these species have been carried out at the same PBE0/cc-pVDZ (Li) + LANL2DZ (I) level of theory.

In LiI, the charge separation is stronger compared to $Li_{13}I$ due to a lower electronegativity of Li, the variation being less significant for the natural charges (Table 3). When another electron is added and $LiI^-$ formed, the negative charge on Li is smaller than that on $Li_{13}$ in $Li_{13}I^-$, as a reflection of the lower EA value of Li. The negative charge on I increases only slightly in $LiI^-$ relative to LiI (especially for the natural-charge case), so the additional electron is localized almost entirely at the Li end of the molecule, similar to the $Li_{13}I$ case. The Li atom, an ultimate non-halogen with a low EA value, still wins the additional electron from iodine and thus demonstrates a super-halogen behavior within LiI. This is due to the charge distribution in the neutral LiI (i.e., $Li^{\delta+}I^{\delta-}$), in analogy with the larger cluster. The Mulliken charges show the same effect, even though somewhat less strongly. According to the above model (section $Li_{13}I$), $EA(I^{\delta-})$ is negative for both Mulliken and natural charges, supporting the preferred location of the additional electron.

The $Li_2I$ case is intermediate between LiI and $Li_{13}I$ in terms of charges (Table 3) as well as binding energies (Table 2). Here the optimized isosceles-triangular geometries of the $Li_2I$ and $Li_2I^-$ ground states are considered. The Mulliken charges in $Li_2I$ approach those in $Li_{13}I$, while the natural-charge values are close to those in LiI. There is thus a trend in the variation of the system parameters with increasing size of the metal moiety, while its super-halogen behavior (in terms of the additional-electron localization) manifests itself at all sizes. The relative values of the negative charges on the metal moieties in $Li_nI^-$ follow the relative EA values of $Li_n$, increasing from $n = 1$ to 2 to 13. The additional-electron localization on Li within LiI and on $Li_2$ within $Li_2I$ is also reflected in their relatively low electron affinities (under 1 eV).

**AlI and $Al_2I$.** In the above sections it is shown that the super-halogen behavior becomes somewhat stronger with increasing lithium-moiety size in $Li_nI$. In order to compare with the case of another metal, here we consider small aluminum moieties (correlating to the real, "permanent" super-halogen, $Al_{13}$).

The charge separation between the metal and halogen moieties in the neutral systems decreases from AlI to $Al_2I$, similar to the lithium case. The separation is, however, smaller than in the corresponding $Li_nI$ (Table 4), considerably for the natural and less significantly for the Mulliken charges. This is consistent with the higher ionization energies of $Al_n$.

In $AlI^-$ and $Al_2I^-$, the negative charge is concentrated on I, but considerably less so than for the lithium case. The negative (natural) charge on the metal moiety increases from $AlI^-$ to $Al_2I^-$, in accord with increasing EA and similar to the Li-based counterparts, and approaches a near-equal share with I in $Al_2I^-$ (for which the natural and Mulliken charges are almost identical). This near-equally shared negative charge does not fit the relative EA values, since that for I is at least twice that for $Al_2$ (predicted, 1.2 eV; experimental, 1.5 eV [2]). The reason is therefore largely the positive-ionic character of the $Al_2$ moiety in $Al_2I$ ($\approx Al_2^{+0.5}I^{-0.5}$ in terms of the natural charges) attracting

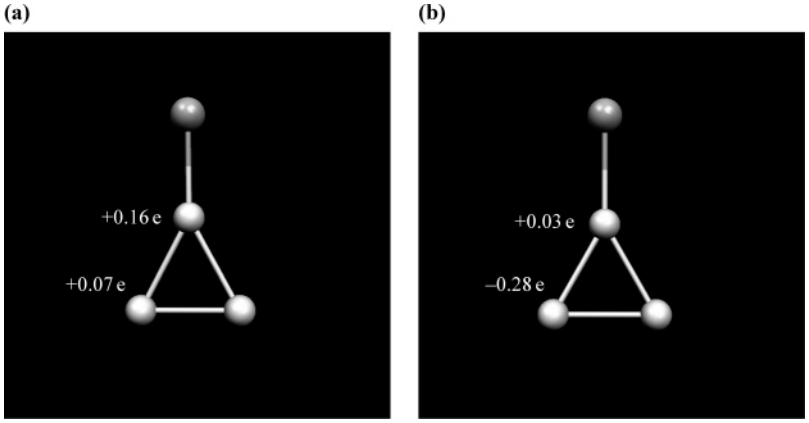


**Figure 2.** Optimized geometries and atomic natural charges of (a) $Al_3I$ and (b) $Al_3I^-$.

the additional electron. Similar to the lithium species, the additional electron is localized almost entirely on the metal moiety, with the Mulliken charges showing a weaker localization. In particular, this is consistent with the relatively low EA values of AlI (0.5 eV) and $Al_2I$ (1.4 eV). Again, the model of section $Li^{13}I$ predicts negative EA for $I^{\delta-}$.

**$Al_3I$.** The rate of the negative-charge accumulation on the metal moiety in $Al_nI^-$ with increasing size (Table 4) suggests crossing the $-0.5$ e level (equal share with iodine) well before $n = 13$. The $Al_3I$ cluster has therefore been studied next. Among its isomers, the most stable one is found to be a $C_{2v}$-symmetric, Y-shaped flat structure with I near the central atom of the isosceles-triangular $Al_3$ (Figure 2). The ground state is predicted to be singlet, with the I-nearest Al distance slightly shorter than in AlI (Table 2) and the Al−Al distances of $2 \times 2.57$ and 2.43 Å, slightly away (up and down) from the (equilateral-triangle) $Al_3$ value of 2.53 Å. The charge separation between the metal and halogen moieties continues to reduce from $Al_2I$ to $Al_3I$ (Table 4) due to increasing electronegativity of $Al_n$, and the Mulliken charges remain more than twice as small as the natural ones. This is reflected in the calculated binding energy of I to $Al_3$ being 10% smaller than for $Al_2I$ (Table 2). The $Al_3I$ dipole moment is calculated to be 2.1 D.

Addition of an electron preserves the general Y-shape of the system while somewhat alters the interatomic distances, slightly stretching that for I-nearest Al (Table 2) and recovering the $Al_3$ moiety to the almost-equilateral triangle with sides of $2.53 \pm 0.02$ Å. The binding energy of $I^-$ to $Al_3$ is $\approx$1 eV smaller than for the neutral counterpart (Table 2), and larger than for $Al_2I^-$ and $AlI^-$ (1.24 eV), likely due to increasing polarizability of the metal moiety. Search for other possible isomers of $Al_3I^-$ is beyond the scope of this work.

As anticipated, the negative charge on the $Al_3$ moiety in $Al_3I^-$ does exceed that on I (Table 4), according to both Mulliken and natural charge distributions (which are close to one another). The $Al_3$ cluster thus demonstrates a full-scale super-halogen behavior within $Al_3I$, similar to $Al_{13}$ within $Al_{13}I$. Unlike for $Al_{13}$, however, this cannot be associated with the higher electron affinity of the isolated metal cluster relative to I, as the EA value of $Al_3$ is calculated to be 1.6 eV (compared to 1.9 eV experimental[16]), significantly lower than the iodine value. The main reason is therefore the predominant attraction of the additional electron to the metal moiety (positively charged within $Al_3I$). This is, in particular, consistent with the EA of $Al_3I$ calculated to be 2.1 eV, close to the value for $Al_3$. The other reason, indeed related to a higher electronegativity of $Al_3$ relative to $Al_2$, is the sufficiently low, $<0.5$ e, positive charge on the metal moiety in $Al_3I$ (to be canceled by the additional electron). Hence, the full-scale super-halogen behavior of $Al_3$ in $Al_3I$ is induced by highly electronegative I creating positive charge on the metal moiety and is also due to its increased EA.

In $Al_3I$, the Al atom nearest to I carries most of the positive charge (Mulliken, $+0.09$ e: natural, $+0.16$ e) and is almost neutralized in $Al_3I^-$, while the two atoms more remote from I accept most of the additional negative charge (Figure 2). This is similar for both Mulliken and natural-charge distributions, and is consistent with the simple picture of the charge−dipole interaction (the additional charge repelling from the negative I).

**$Al_{13}I$.** In order to complete the comparison with the Al-based species, the $Al_{13}I$ cluster is considered as well. Its and $Al_{13}I^-$ structures have been predicted earlier[8] and are reproduced here at the uniform level of theory applied throughout this work. The optimized geometries are shown in Figure 3 and parametrized in Table 2, and the charges are given in Table 4.

In $Al_{13}I$, the charge separation between the metal and halogen moieties is relatively small (less than in $Al_3I$), unlike in $Li_{13}I$, as a consequence of the higher electronegativity of $Al_{13}$ compared to $Li_{13}$. In particular, this is consistent with the calculated binding energy of I to $Al_{13}$ which is significantly less than for $Li_{13}I$ as well as for $Al_3I$ (Table 2). The decrease of the I:$Al_n$ binding with increasing $n$ is opposite to the $Li_nI$ case. The metal moiety in $Al_{13}I$ is positively charged; therefore, in spite of EA of $Al_{13}$ exceeding that of iodine, the latter is still more electronegative, apparently due to its significantly higher ionization energy. The dipole moment of $Al^{13}I$ is, however, very small, $\approx$0.04 D, unlike for smaller clusters as well as for $Li_{13}I$.

As another result of the reduced charge separation, and again due to the dominant attraction of the additional electron to the positively charged metal moiety, the negative charge in $Al_{13}I^-$ concentrates mainly on $Al_{13}$ (Table 4), similar to the $Al_3I^-$ case and different from $Li_{13}I^-$. The present results for the charges in $Al_{13}I$ and $Al_{13}I^-$ are very close to the data reported previously,[8,14] and the Mulliken and natural charges are really close to one another in these systems. The trend of increasing negative charge on the metal moiety with its size continues from $Al_3I^-$ to $Al_{13}I^-$.

Due to the EA value of $Al_{13}$ exceeding that of I, the calculated binding energy of $I^-$ to $Al_{13}$ is larger than that of I to $Al_{13}^-$ (Table 2), these two values being respectively somewhat higher and lower than the above I:$Al_{13}$ value. The increase of the binding energy between the halogen and (neutral) metal moieties from the neutral to the ionic system is opposite to its reduction for smaller clusters as well as for the lithium-based case. However, it is consistent with the binding energy variations with increasing cluster size, a decrease for the neutral and an increase

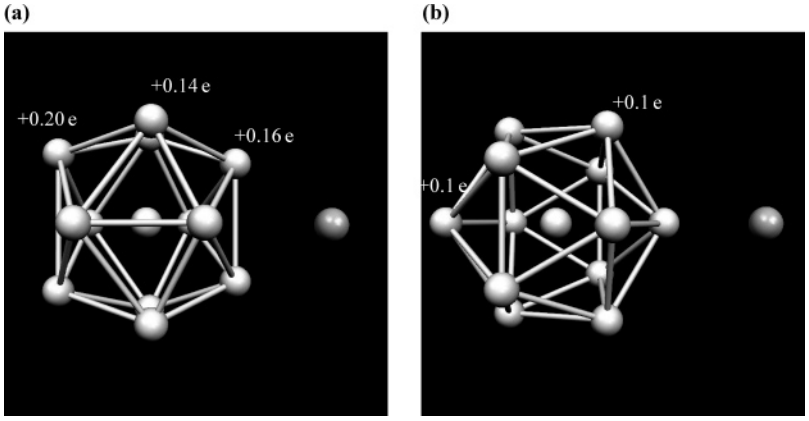


**Figure 3.** Optimized geometries and atomic natural charges of (a) $Al_{13}I$ and (b) $Al_{13}I^-$.

for the ionic systems, so that the two sets intersect at some intermediate size between $n = 3$ and 13. A more precise determination of this intersection is beyond the scope of the present work.

Concerning other features of the predicted charge distribution, the Al atom in the center of the $Al_{13}$ moiety in $Al_{13}I$ carries a (natural) charge of $-1.62$ e, i.e., more than twice the value for $Li_{13}I$. The positive charge is distributed over the $Al_{13}$ cluster periphery much more evenly (Figure 3a) than in the Li-based counterpart, the two Al atoms most remote from I being most positive. In isolated $Al_{13}$, the central-atom charge is $-1.71$ e. Unlike in the Li-based system, the corresponding Mulliken charges in $Al_{13}I$ are quite reasonable, with $Al_{center}$ charged to $+0.41$ e and with the peripheral atoms slightly negative (up to $-0.07$ e). Essentially the same description (except for a more symmetric peripheral charge) applies to isolated $Al_{13}$, which is thus relatively weakly perturbed by I within $Al_{13}I$ (true also for the natural charges).

In $Al_{13}I^-$, the central Al atom is slightly less negatively natural-charged ($-1.44$ e) than in $Al_{13}I$, in accord with its somewhat reduced charge ($-1.51$ e) in isolated $Al_{13}^-$ relative to $Al_{13}$. This is different from the increased charge on $Li_{center}$ in $Li_{13}I^-$ relative to $Li_{13}I$. Besides, the peripheral Al atoms in $Al_{13}I^-$ remain slightly positive (Figure 3b). In terms of the Mulliken charges, however, $Al_{center}$ is more positive ($+0.63$ e), and the periphery is, accordingly, more negative in $Al_{13}I^-$ than in $Al_{13}I$. By comparison, $Al_{center}$ in isolated $Al_{13}^-$ is slightly less charged ($+0.56$ e). So again the influence of I is rather weak.

The negative-charge concentration on the opposite side of $Al_3I^-$ from I (section AlI and $Al_2I$) resembles the HOMO density in $Al_{13}I^-$ concentrating on the Al atom most remote from iodine.[8] Indeed, the additional electron in both $Al_3I^-$ and $Al_{13}I^-$ occupies HOMO, so the additional-charge distribution does describe the HOMO density. In $Al_{13}I^-$ the additional negative-charge portion going to the Al atom on the opposite end of the cluster from I is the largest ($-0.3$ e), consistent with this atom being most positive ($+0.4$ e) in $Al_{13}I$ (when frozen in the geometry of $Al_{13}I^-$) and with the repulsion of the additional electron from $I^{\delta-}$.

It should be noted once again that while the Mulliken and natural *overall* charges on $Al_{13}$ are nearly identical in $Al_{13}I$ as well as in $Al_{13}I^-$, they correspond to a positive or negative central Al atom in the $Al_{13}$ moiety, respectively. The Mulliken version in this case appears to better fit the physical intuition, while suffering from the instability of the predicted charge values with respect to the level of accuracy. In particular, these values may vary appreciably for different DFT functionals, for instance B3LYP relative to PBE (the former showing the positive charge on the central Al atom in $Al_{13}I$ twice as large).

## Conclusions

An ab initio investigation of $Li_{13}I$ and $Li_{13}I^-$ clusters has been performed at a DFT level of theory, and charge distributions analyzed at both the Mulliken and natural-charge levels. A comparison is made with smaller $Li_nI$ species and Al-based analogues.

Optimized structures for both $Li_{13}I$ and $Li_{13}I^-$ show the iodine atom located at the hollow site between three Li atoms and the metal moiety generally preserving the icosahedral shape of the isolated $Li_{13}$ cluster. Different spin states do, however, influence its geometry for the neutral system, varying from slightly elongated (in the direction of the I atom) for the ground triplet state to significantly compressed (by $\approx$10%) for the singlet state, with the dipole moment remaining unchanged. The ionic system shows only a weak perturbation of the metal moiety shape.

The Mulliken and natural charge distributions in $Li_{13}I^{(-)}$ (as well as $Li_{13}^{(-)}$) exhibit excessively positive and (unexpectedly) negative central Li atom, respectively, and oppositely charged periphery of the $Li_{13}$ moiety which is overall positive in both cases. The natural charges on the lithium and iodine moieties are significantly larger (in absolute value). Both methods agree that in $Li_{13}I^-$ the additional electron is localized predominantly on the metal moiety which is positively charged in the neutral system. This is consistent with the anticipated charge−dipole interaction. The same feature is present in smaller species, LiI and $Li_2I$. The alkali-metal components thus exhibit a super-halogen behavior in terms of winning the additional electron from the halogen atom in $Li_nI^-$, even though isolated $Li_n$ are no super-halogens with low electron affinities.

A simple model interpretation is developed in terms of the metal and halogen moieties carrying charges within the system (i.e., $Li_{13}I = Li_{13}^{\delta+}I^{\delta-}$) and therefore having effective electron affinities (EA) very different from those for the isolated (neutral) components. Because these charges are due to the higher electronegativity of iodine, the super-halogen behavior of the metal moiety is induced by the halogen atom.

For a small enough partial charge ($\delta$ value) in the neutral system the additional electron (in the ionic system) still localized mainly on the metal moiety can make it more negative than iodine. This happens in $Li_{13}I$ and even $Li_2I$ according to the Mulliken charges but does not with the natural charges (corresponding to larger $\delta$).

Comparison with the aluminum-based counterparts confirms the above considerations. The natural charges are smaller in

$Al_nI$ than in $Li_nI$ due to higher EA of $Al_n$, and decrease with increasing $n$, so the metal moiety in $Al_nI^-$ accumulates negative charge more quickly with cluster size, exceeding the equal share with iodine at $n = 3$. The Mulliken charges are close to the natural charges in the $Al_nI^-$ clusters. The $Al_3$ moiety thus exhibits a full-scale super-halogen behavior within $Al_3I$ and is more negative than I in $Al_3I^-$, even though EA of isolated $Al_3$ is considerably smaller than that of isolated I.

A more metal-concentrated distribution of the negative charge in $Al_{13}I^-$ has been predicted previously[8] and associated with EA of isolated $Al_{13}$ exceeding that of isolated I (hence making the metal cluster a real super-halogen). Present results indicate that this is also due to the positive $Al_{13}$ moiety in neutral $Al_{13}I$, hence due to the presence of I.

The observed trends suggest that $Al_n$ ($n > 3$) moieties in $Al_nI^-$ can be expected to behave like $Al_3$ and to be more negative than iodine even though their EA are smaller.[2]

The discussed phenomena can be used in analysis of other aluminum−halide clusters such as $Al_{13}X^{(-)}$ (X = Br, Cl, F) showing an increasing additional-electron loss by the metal moiety to the increasingly electronegative halogen moiety.[17]

Similar induced electron affinities and associated charge distributions are likely to be found in other cluster systems with components of different electronegativities. One example is $Al_{13}H^-$, with the extra negative charge carried entirely by the metal moiety, apparently due to the negatively charged H atom in $Al_{13}H$ [18] (similar to the $Al_{13}I^{(-)}$ case).

Knowledge of these properties is important for constructing materials from such systems as building blocks, in particular for a proper choice of counter ions in ionic crystals. The fusion of the metal clusters within a material could be prevented (besides their Coulomb repulsion) by appropriate spacers, such as ligands or maybe sufficiently large counter ions (perhaps other clusters).

**Note Added in Proof.** After this paper was submitted, new results were published by Y.-K. Han and J. Jung for the $Al_{14}I^-$ cluster (*J. Chem. Phys.* **2006**, *125*, 084101). They predict a charge of −0.70e on the aluminum moiety (very close to our value for $Al_{13}I^-$), even though EA($Al_{14}$) is much lower than EA(I). This thus further supports our predictions. Han and Jung also state that the jellium model may be inappropriate for such clusters. This is supported by our finding of the triplet rather than singlet ground state for $Li_{13}I$, which has 20 valence electrons from its atoms.

**Acknowledgment.** The authors acknowledge the technical assistance of Dr. Thomas Hu regarding the UOIT/Science computing facilities administration. A part of the calculations has been performed using the computing facilities in the University of Toronto/Department of Chemistry. H.L. is grateful to the UOIT for the Undergraduate Summer Research Award.

## References and Notes

(1) Alonso, J. A. *Chem. Rev.* **2000**, *100*, 637.
(2) Li, X.; Wu, H.; Wang, X.; Wang, L. *Phys. Rev. Lett.* **1998**, *81*, 1909.
(3) Taylor, K. J.; Pettiette-Hall, C. L.; Cheshnovsky, O.; Smalley, R. E. *J. Chem. Phys.* **1992**, *96*, 3319.
(4) Zhai H.-J.; Li, J.; Wang, L.-S. *J. Chem. Phys.* **2004**, *121*, 8369.
(5) Gutsev, G. L.; Boldyrev, A. I. *Chem. Phys.* **1981**, *56*, 277.
(6) Wang, X.-B.; Ding, C.-F.; Wang, L. S.; Boldyrev, A. I.; Simons, J. *J. Chem. Phys.* **1999**, *110*, 4763.
(7) Elliott, B. M.; Koyle, E.; Boldyrev, A. I.; Wang, X.-B.; Wang, L.-S. *J. Phys. Chem. A* **2005**, *109*, 11560.
(8) Bergeron, D. E.; Castleman, A. W., Jr.; Morisato, T.; Khanna, S. N. *Science* **2004**, *304*, 84; *J. Chem. Phys.* **2004**, *121*, 10456.
(9) Aprà, E.; Windus, T. L.; Straatsma, T. P.; Bylaska, E. J.; de Jong, W.; et al. *NWChem A Computational Chemistry Package for Parallel Computers*, Version 4.7; Pacific Northwest National Laboratory: Richland, WA, 2005. http://www.emsl.pnl.gov/docs/nwchem/.
(10) Flükiger P.; Lüthi, H. P.; Portmann, S.; Weber, J. *MOLEKEL 4.0*; Swiss Center for Scientific Computing: Manno, Switzerland, 2000. http://www.cscs.ch/molekel/.
(11) Schultz, N. E.; Staszewska, G.; Staszewski, P.; Truhlar, D. G. *J. Phys. Chem. B* **2004**, *108*, 4850.
(12) *NIST Chemistry WebBook*; NIST Standard Reference Database No. 69, June, 2005 Release. http://webbook.nist.gov/chemistry/.
(13) Fournier, R.; Cheng, J. B. Y.; Wong, A. *J. Chem. Phys.* **2003**, *119*, 9444.
(14) Han Y.-K.; Jung, J. *J. Chem. Phys.* **2004**, *121*, 8500.
(15) Autschbach, J.; Hess, B. A.; Johansson, M. P.; Neugebauer, J.; Patzschke, M.; Pyykkö, P.; Reiher, M.; Sundholm, D. *Phys. Chem. Chem. Phys.* **2004**, *6*, 11.
(16) Wu, H.; Li, X.; Wang, X.-B.; Ding, C.-F.; Wang, L.-S. *J. Chem. Phys.* **1998**, *109*, 449.
(17) Jung, J.; Kim, J. C.; Han, Y.-K. *Phys. Rev. B* **2005**, *72*, 155439.
(18) Han, Y.-K.; Jung, J.; Kim, J. C. *J. Chem. Phys.* **2005**, *122*, 124319.